Six States Switching of Redox-Active Molecular Tweezers by Three Orthogonal Stimuli

Benjamin Doistau, Lorien Benda, Jean-Louis Cantin, Lise-Marie Chamoreau, Eliseo Ruiz, Valérie Marvaud, Bernold Hasenknopf, Guillaume Vives

Six states switching of redox-active molecular tweezers by three orthogonal stimuli

Benjamin Doistau, Lorien Benda, Jean-Louis Cantin, Lise-Marie Chamoreau, Eliseo Ruiz, Valerie Marvaud, Bernold Hasenknopf, Guillaume Vives

Six states switching of redox-active molecular tweezers by three orthogonal stimuli

Benjamin Doistau,[†] Lorien Benda,[†] Jean-Louis Cantin,[‡] Lise-Marie Chamoreau,[†] Eliseo Ruiz,[§] Valérie Marvaud,[†] Bernold Hasenknopf,[†]* Guillaume Vives[†]*

[†] Sorbonne Universités, UPMC Univ Paris 06, CNRS, Institut Parisien de Chimie Moléculaire, UMR 8232, 4 place Jussieu, 75005 Paris (France)

[‡] Sorbonne Universités, UPMC Univ Paris 06, INSP, 4 place Jussieu, 75005 Paris (France)

[§] Departament de Química Inorgànica and Institut de Recerca de Química Teòrica i Computacional, Universitat de Barcelona, Diagonal 645, E-08028 Barcelona, Spain

ABSTRACT: A six level molecular switch based on terpyridine(Ni-salphen)$_2$ tweezers and addressable by three orthogonal stimuli (metal coordination, redox reaction and guest binding) is reported. By a metal coordination stimulus, the tweezers can be mechanically switched from an open "W"-shaped conformation to a closed "U"-shaped form. Theses two states can each be reversibly oxidized by the redox stimulus and bind to a pyrazine guest resulting in four additional states. All six states are stable and accessible by the right combination of stimuli and were studied by NMR, XRD, EPR spectroscopy and DFT calculations. The combination of the supramolecular concepts of mechanical motion and guest binding with the redox non-innocent and valence tautomerism properties of Ni-salphen complexes added two new dimensions to a mechanical switch.

INTRODUCTION

Molecular machines have recently attracted an increasing interest due to their promising abilities to control matter at the molecular scale.[1] Among the large variety of mechanical machines,[2] molecular switches[3] using mechanical motion in response to external stimuli can be considered as important precursors. Beyond switches based on bi-stable systems, the introduction of multistate systems may be necessary to develop multifunctional devices.[4] For example, molecular computing could, in principle, profit from ternary or higher-order digit representations to enable smaller devices. Despite this obvious interest, molecules that can exist in more than two stable and independently addressable states remain largely unexplored.[5] In particular, examples of six-level molecular switches are scarce in the literature and the only examples have been obtained by combining a photochromic unit with redox or pH-sensitive active units. [5a, 5c, 5d] While photo- and electro-induced processes have received much attention as modes of switching, multistate switching by those stimuli is difficult to implement, as it requires selective excitation of more than two units, and therefore designing of multiple modules without excitation overlap. In this regard, using a coordination based mechanical switch is an interesting approach since it enables addressability by the design of the coordination sites with total conversion and thermal stability[6] that can be difficult to achieve with photochromic systems.

We are interested in using the mechanical motion of switchable molecular tweezers[7] to control properties at the molecular level. Our system is based on a terpyridine ligand functionalized in 6 and 6" positions by salphen complexes. The open tweezers adopts a 'W' shaped conformation that can be switched to a closed 'U' one by a coordination stimulus bringing in proximity the two functional salen complexes. By using platinum or copper salphen complexes a modulation of the luminescence[8] and magnetic[8b] properties respectively was achieved demonstrating the versatility of such mechanical

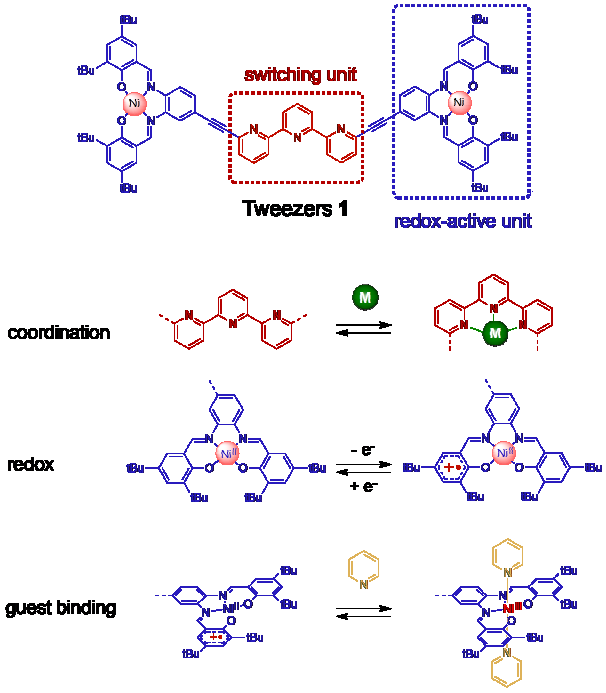

Figure 1: Redox-active molecular tweezers **1** and effect of the 3 orthogonal stimuli (coordination, redox and guest binding).

switch. We wished to exploit the modularity of our platform to combine ion triggered mechanical motion with redox activity and substrate binding in order to achieve a multi-state switch. Ni-salphen complexes were chosen as functional units since the salphen ligand in such case are known to be non-innocent with reversible oxidation properties.[9] Furthermore, upon one electron oxidation a valence tautomerism can be observed between Ni^{III}-salen and Ni^{II}-salen^{+} species in the presence of pyridine ligands enabling an additional orthogonal stimulus.[10] Herein we describe the synthesis of terpy (Ni-salphen)$_2$ tweezers (Figure 1) and the study of their six-level switch by using three orthogonal stimuli: i) metal coordination of the terpyridine moiety to open/close the tweezers ii) reversible oxidation of the Ni-salphen complexes and iii) guest binding to oxidized Ni-salphen coupled to valence-tautomerism.

RESULTS AND DISCUSSION

Synthesis. Tweezers **1** were synthetized by a modular approach using a "chemistry on complex" strategy exploiting the inertness of Ni-salphen complexes (Scheme 1) to perform a double Sonogashira coupling between alkyne Ni-salphen complex **6** and 6,6'' dibromo-terpyridine **7** as key step. Ni-salphen complex **4** was first obtained by a one-pot condensation between salicylaldehyde **3** and 4-bromo-1,2-diaminobenzene using Nickel acetate as a template. The aryl bromide was then reacted with trimethylsilylacetylene (TMSA) in a Sonogashira coupling reaction to yield after deprotection complex **6**. After a final double coupling with **7**, tweezers **1** were obtained and fully characterized by NMR spectroscopy and mass spectrometry. This modular strategy and the inert nature of the Nickel-salphen complexes enabled a perfect control the coordination of the two binding sites (salphen and terpyridine). The absence of correlation in the NOESY spectra between H_2 and H_3 (Figure S2) is in agreement with an *s*-trans 'W' shaped conformation of the terpy in solution due to the repulsion between the nitrogen lone pairs.

Scheme 1: Synthesis of Tweezers 1.

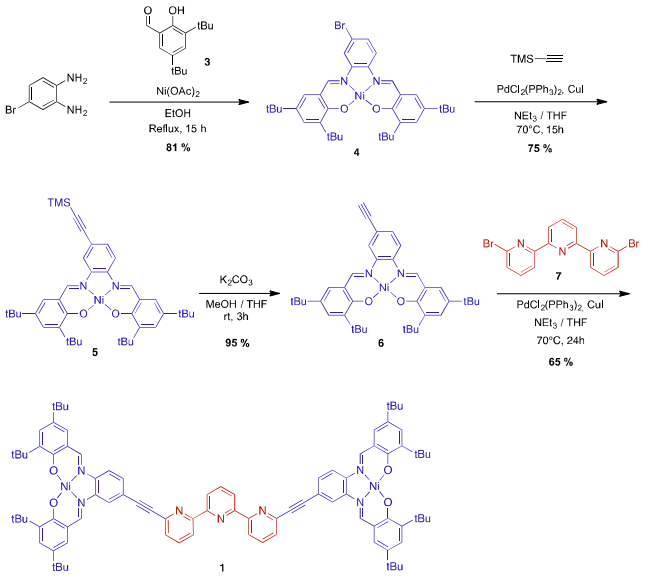

A model mono substituted terpy(Ni-salphen) **2** tweezers was also synthetized using less equivalent of alkyne complex **6** for the Sonogashira coupling reaction with **7**. In this case, single crystals could be obtained by slow evaporation from a $CHCl_3$ solution (Figure 2). Half-tweezers **2** crystallize in orthorhombic space group $Pca2_1$ (a = 41.7129(8), b = 7.09050(10), c = 17.3156(3) Å, α = β = γ = 90°). The molecule adopts in the solid state a coplanar geometry between the terpy unit and Ni-salphen with a full conjugation of the π system. As expected the terpy also adopts an *s*-trans geometry and the Nickel complex is square planar resulting in a diamagnetic low spin d^8 configuration enabling NMR studies.

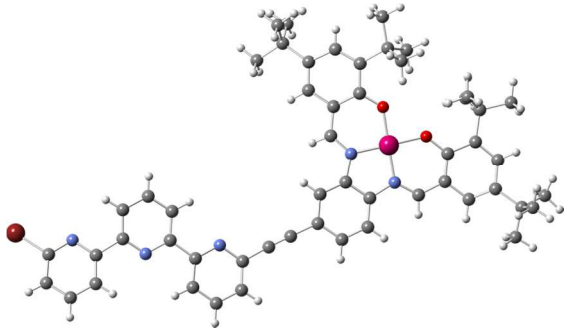

Figure 2: Crystal structure of half tweezers **2**.

Coordination stimulus. The mechanical switching between the open and closed form for tweezers **1** in the neutral form (coordination stimulus **a**) was first studied by NMR titration. Upon addition of $ZnCl_2$ the ^{1}H NMR spectra (Figure 3) showed a progressive disappearance of the open tweezers signals and the appearance of a new set of peaks corresponding to the closed conformation in slow exchange on the NMR timescale. The closing reaction can be easily monitored by the growth of a shielded doublet at 6.3 ppm and a strongly deshielded singlet at 9.0 ppm corresponding to phenyl proton H_7 and H_6 respectively highlighting aromatic anisotropic effects due to the spatial proximity of the two Ni-salphen moieties in the closed form. After addition of 1 eq of $ZnCl_2$ the tweezers are fully closed and the formation of the 1:1 complex was confirmed by 2D NMR with a NOE correlation peak between H_2 and H_3 (Figure S3) and by mass spectrometry (Figure S4) with a molecular ion peak at 1568.6 *m/z* corresponding to $[Zn(\mathbf{1})Cl]^+$. ^{1}H NMR DOSY experiments were performed (at 4×10^{-4} mol.L^{-1} in $CDCl_3$ at 300K) to evaluate the effect of shape change on the diffusion coefficient. The diffusion coefficients of the open **1** and closed $[Zn(\mathbf{1})]Cl_2$ tweezers are quite similar ($2.45\ 10^{-9}$ and $2.15\ 10^{-9}$ m^2.s^{-1} respectively) with a rather counter-intuitive slightly faster diffusion for the extended-disk-shaped open tweezers than the more spherical closed tweezers conformation.[11] This effect is probably due to the increase of the solvation shell around the molecule and thus of its hydrodynamic radius upon addition of the zinc(II) salt.

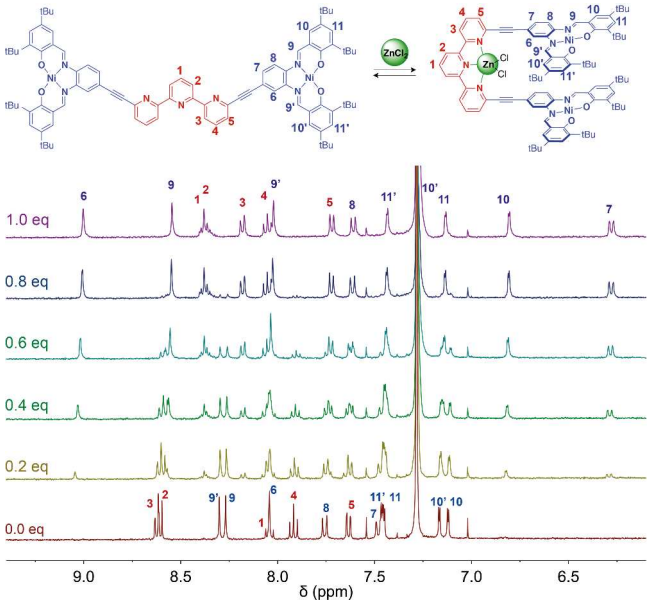

Figure 3: ^{1}H-NMR (400 MHz) titration of tweezers **1** with $ZnCl_2$ in $CDCl_3$ at 300 K.

The closing of the tweezers was also monitored by a UV-Vis titration with $ZnCl_2$ (see Figure S6). The spectra presented a single evolution up to one equivalent of zinc with isosbestic points (at 552, 482, 434, 378 and 354 nm) indicating the exclusive formation of the $[Zn(\mathbf{1})]Cl_2$ complex. Titration with $Zn(ClO_4)_2$ displayed the same behavior demonstrating no dependency on the counter ions (see Figure S7). The titration curves were fitted by a 1:1 binding model and revealed in both cases a strong binding constant (log K > 7). Single crystals of closed tweezers $[Zn(\mathbf{1})]Cl_2$ suitable for X-ray diffraction were obtained by slow evaporation (Figure 4). $[Zn(\mathbf{1})]Cl_2$ crystalized in monoclinic space group I2/a, with a unit cell of 20286.8(6) Å^3 (a = 35.3839(4), b = 11.1376(2), c = 51.7427(9) Å, α = γ = 90°, β = 95.8060(10)°). Each Ni-salphen unit adopts a square planar geometry with average Ni-O and Ni-N distances of 1.851 and 1.853 Å respectively characteristic of Ni-salen complexes.[9b] The tweezers present an helicoidally shaped geometry that brings in close proximity the two Ni-salphen units with a Ni-Ni distance of 4.820 Å. The reversibility of the motion was then obtained by adding tris(2-aminoethyl)amine (tren) as a competitive ligand that can selectively remove the zinc without decoordinating the Ni-salphen complexes. The titration was followed by NMR (Figure S5) and showed the disappearance of the closed tweezers protons and the recovery of the open conformation after addition of around 1 eq of tren demonstrating the reversibility of the mechanical switch.

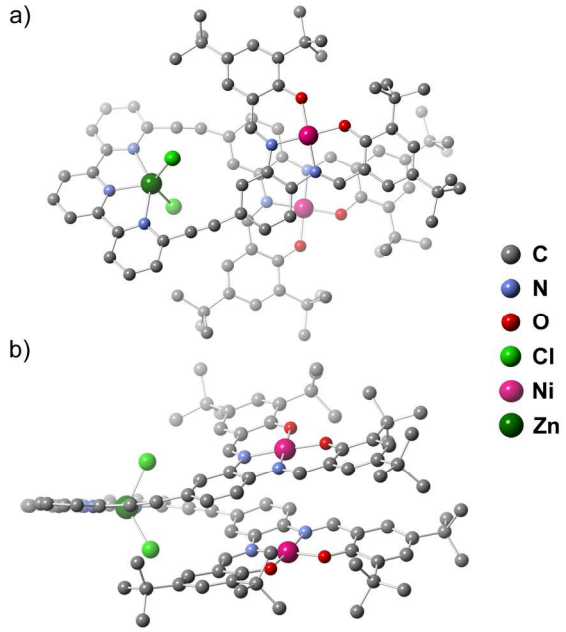

Figure 4: Crystal structure of closed tweezers $[Zn(\mathbf{1})]Cl_2$.

Redox stimulus. Ni-salen complexes are known to present redox non-innocent properties,[9] ie upon oxidation the complex presents valence tautomerism with a ligand centered oxidation at room temperature that can switch to a metal centered oxidation at very low temperature.[12] More interestingly, this tautomerism can be promoted by the coordination of an apical ligand such as pyridine that can result in an exclusive Ni^{III} species.[10] These subtle electronic properties of the Ni-salphen moieties were taken advantage of to add two other dimensions to the switching mechanism of the tweezers.

The electrochemical properties of the tweezers were studied by cyclic voltammetry (CV) and differential pulse voltammetry (DPV) (Figure 5). CV of the open tweezers displays two successive reversible two-electrons redox waves (0.97 and 1.33 V/SCE) corresponding to the formation of $\mathbf{1}^{2+}$ and $\mathbf{1}^{4+}$ species respectively (Figure 5c Edge **b**). The two oxidations are observed at potentials similar to the one of Ni-salphen complex **4** (0.96 and 1.33 V/SCE) indicating that both oxidations are centered on the Ni-salphen moieties as described in the literature.[9b, 9c] The simultaneous oxidation of both Ni-salphen indicates no electronic interaction between the two redox-active moieties in the open conformation, which is expected despite a conjugated pathway from the large distance between them (~20 Å). Upon closing by addition of $ZnCl_2$, the first oxidation wave is clearly split in two reversible waves at 0.92 and 1.08 V/SCE. This splitting effect is also observed with $Zn(ClO_4)_2$ as Zn^{2+} source (with potentials at 0.94 and 1.06 V/SCE see Figure S8) indicating no significant effect of the counter anion on the electrochemical behavior of the closed tweezers. The first oxidation potential value is shifted by 50 mV to lower potential compared to the open conformation. This effect can be attributed to the coordination of the terpy by Zn^{2+} that results in back-donation of the zinc to the π system[13] as observed on a model half-tweezers terpy-(Ni-salphen) where zinc coordination has the same effect (Figure S9). However, the splitting can be attributed to the interaction between the two Ni-salphen units that are in close spatial proximity in the closed conformation. To discriminate between electronic coupling or electrostatic effects, spectro-electrochemisty experiments were performed. The monitoring

of the UV-Vis and NIR spectra upon electrolysis presented no significant difference in the NIR region between the open and closed conformation with, in both cases, the appearance of a broad intervalence band centered around 900 nm corresponding to the intra-complex transition usually observed in Ni-salen complexes[9a, 14] (see Figure S11-12). This indicates that the splitting of the first oxidation wave is probably due to an electrostatic effect. The proximity of the positive charge generated upon oxidation of one Ni-salphen renders the oxidation of the second one more difficult (Figure 5c Edge **b'**) as already observed in multi-ferrocenyl systems.[15]

Oxidized open tweezers $\mathbf{1}^{2+}$ were then generated by bulk electrolysis (at 1.2 V vs SCE) of a solution of tweezers **1**. Opening and closing of the oxidized tweezers were performed by successive addition of $Zn(ClO_4)_2$ and excess (10 eq) terpyridine demonstrating the reversible switching along Edge **a'** (Figure 5c). The switching was monitored *in situ* by DPV (scanning from 1.2 to 0 V) with the appearance of the characteristic splitting of the first reduction wave in the closed form after addition of $Zn(ClO_4)_2$; and recovery of the single reduction wave for both salphen units that is characteristic of the open form after addition of terpyridine (see Figure S10). It should be noted that $Zn(ClO_4)_2$ was preferred as closing stimulus in this case to avoid potential reduction of the oxidized species by the chloride ions of $ZnCl_2$. Tren ligand could not be used in this case to selectively reopen the oxidized tweezers as it also reduced the tweezers. It can nevertheless be considered as a combined agent that can directly reset the system to the open form **1** (Stimuli **a** + **b**). Thus two additional states of the molecular switch system are accessible by oxidation.

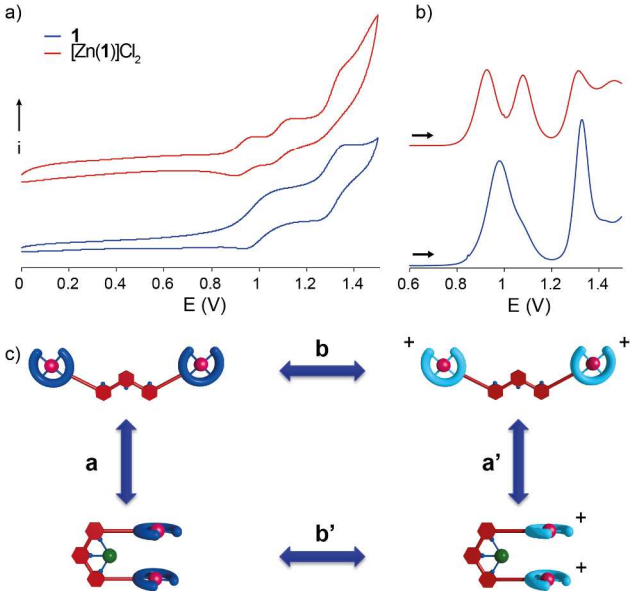

Figure 5: a) CV and b) DPV of open and closed tweezers on Pt working electrode in CH_2Cl_2 (2.0×10^{-4} M) with $TBAPF_6$ (0.1 M). Scan rate: 20 $mV.s^{-1}$, potentials are recorded versus SCE; c) schematic representation of the four states accessible by the coordination and redox stimuli.

Guest binding stimulus. An additional orthogonal stimulus was then used to add another dimension of switching. Indeed pyridine has been described to promote a geometry change from square planar to octahedral by coordinating Ni in apical position after oxidation of the complex. Thus the effect of pyrazine on $\mathbf{1}^{2+}$ was studied by EPR to provide an accurate insight on the location of the unpaired electrons.

X-band EPR spectrum of open tweezers $\mathbf{1}^{2+}$ (Figure 6a) in frozen CH_2Cl_2 (+ 0.1 M $TBAPF_6$) solution at 20 K displays two rhombic signals at g_{av} values of 2.23 and 2.03 that can be respectively attributed to a ligand radical and low spin Ni^{III} species according to the literature.[9b, 10, 16] The ligand centered radical rhombic signal is characteristic of the presence of excess supporting electrolyte ($TBAPF_6$).[16b] As previously observed,[16b] the signal corresponding to Ni^{III} became less intense at higher temperature (see Figure S13 at 100 K) suggesting a valence tautomerism depending on the temperature. In presence of an excess of pyrazine a characteristic low spin Ni^{III} signal with hyperfine splitting is observed for $\mathbf{1}^{2+}$ (Figure 6b). The presence of a well-resolved quintuplet in the high-field component (g = 2.03) is indicative of the existence of an octahedral Ni^{III} complex with two equivalent pyrazine ligands axially bonded (Figure 6 Edge **c**).[10] The spectrum is very similar to isolated Ni-salen$^+$ complexes indicating that the two Ni-salphen moieties in the tweezers are not interacting. The coordination of the pyrazine ligands seems thus unable to trigger a closing of the tweezers by the establishment of a bridging pyrazine between the to Ni centers.

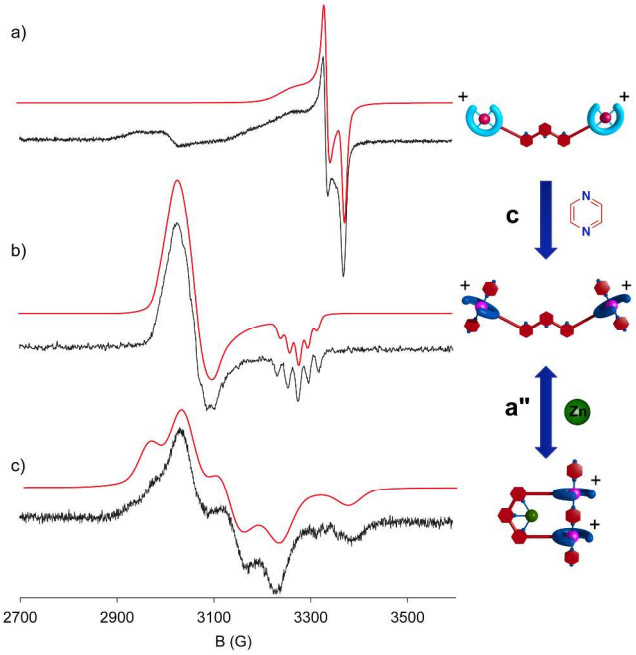

Figure 6: X-band EPR spectrum of oxidized (a) open tweezers $\mathbf{1}^{2+}$ (b) $\mathbf{1}^{2+}$ with 100 eq. of pyrazine and (c) closed tweezers $[Zn(\mathbf{1})]^{4+}$ with 100 eq. of pyrazine in frozen solution of CH_2Cl_2 (1.0×10^{-4} $mol.L^{-1}$ + 0.1 M $TBAPF_6$) at 20 K (black); theoretical fit (red).

However upon addition of zinc(II) a drastic change in the EPR spectra was observed (Figure 6c) (Edge **a''**). The signal was fitted by a S = 1 spin system corresponding to the two ½ spins located on the Ni^{III} in exchange and dipolar coupling interactions, yielding to the formation of two new spin state S = 0 and S = 1. The fit gave access to the g values (g_x = 2.230; g_y = 2.160; g_z = 2.027) and to the dipolar zero field splitting parameter (D = 183 MHz). In order to discriminate between through space interaction between the two Ni-salphen moieties and through ligand interaction by a bridging pyrazine a control experiment in presence of pyridine was conducted. The EPR spectra of $[Zn(\mathbf{1})]^{4+}$ in presence of pyridine is very different from the one with pyrazine and is similar to the open tweezers in presence of pyrazine (Figure S14). Since pyridine cannot play the role of bridging ligand and only coordinate the Ni in

apical position we can assume that in the closed tweezers one pyrazine ligand bridges the two Ni centers by an allosteric effect, and enables a through ligand exchange interaction (Figure 8 Edge **c'**). As single crystals for diffraction studies could not be obtained, DFT calculations were then performed (FHI-aims code[17] with PBE functional[18] and numerical tight basis set, for more details see Computational details in Supporting Information) to confirm the location of the pyrazine. The accuracy of such methodology has been verified by comparison with the experimental structure of the $[Zn(\mathbf{1})]Cl_2$ complex (Figure S17). An optimized structure of $[Zn(\mathbf{1})pz_3Cl_2]^{2+}$ was obtained showing the tweezers in a folded geometry similar to the one in the crystal structure but with a larger intramolecular Ni-Ni distance of 7.10 Å (Figure 7). The flexibility of the alkyne spacers allows this distortion and enables the bridging position of one pyrazine.

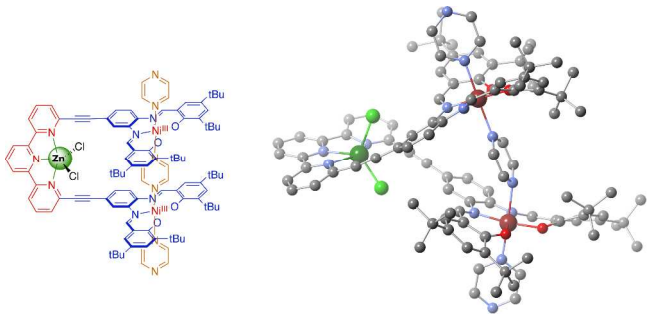

Figure 7: Optimized structure of $[Zn(\mathbf{1})pz_3Cl_2]^{2+}$ using the PBE functional with the FHI-aims code.

To have a better insight on ground state spin value in the closed form, the exchange coupling constant was evaluated from the evolution of the intensity of the EPR signal as a function of temperature. The integration curve decreased at low temperature corresponding to an antiferromagnetic coupling between the two spin centers, indicating a S = 0 fundamental state. By fitting with a two-level Boltzmann model (Figure S16) a value of J = -2.4 cm^{-1} was obtained. This behavior was corroborated by calculations with the B3LYP functional[19] using optimized structure shown in Figure 7 yielding a calculated J value[20] of -2.3 cm^{-1} in excellent agreement with the experimental data (see Supporting Information for more details). Thus, the pyrazine stimulus enables two new accessible states that can be monitored by EPR. We noticed that in absence of pyrazine, the EPR spectra (Figure S15) of $[Zn(\mathbf{1})]^{4+}$ presents no through space interactions mainly due to the spin delocalization on the Ni-salen ligand as confirmed by DFT calculations with only a 0.12 spin density on the Nickel atoms in contrast to 0.97 in $[Zn(\mathbf{1})pz_3]^{4+}$. Hence, the coordination of the pyrazine ligand in the oxidized state has a drastic effect on the electronic properties of the system by shifting the radical location from Ni^{II}-phenoxyl to Ni^{III}-phenoxide and enabling a through ligand magnetic coupling in the closed form. The pyrazine can be removed after reduction since no apical binding on the Ni-salphen complex was observed for the neutral tweezers. Thus the reduction stimulus acts as a reset of the system enabling the recovery of unbound tweezers **1**.

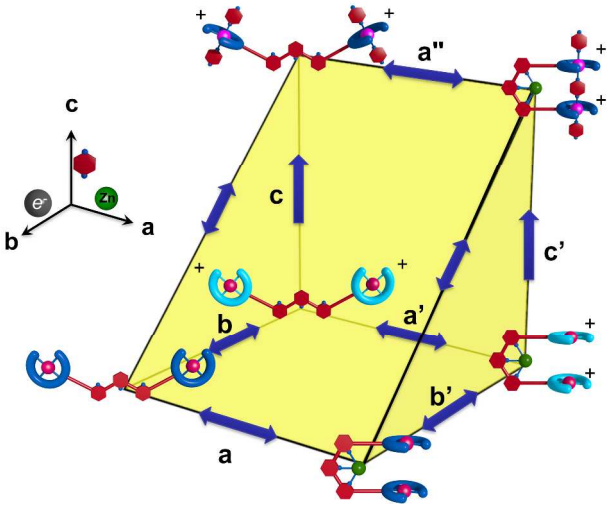

Figure 8: Representation of the six-level switching with 3 orthogonal stimuli (coordination, redox and guest binding).

CONCLUSION

In summary, by combining three orthogonal stimuli (redox, coordination, guest binding) a remarkable six-states multifunctional switching system was achieved that can be represented in 3D as a truncated cube (Figure 8) with each stimulus along one axis. The metal coordination stimulus (axis **a**) enables a mechanical closing of the neutral and oxidized open states (edges a, a', a"). The switching along theses edges is reversible upon addition of a competitive ligand such as tren or terpyridine. The orthogonal redox stimulus (axis **b**) triggers a reversible oxidation of the open or closed tweezers (axis **b**) adding two new accessible states along edge b and b'. Finally, the orthogonal pyrazine binding stimulus (axis **c**) enable two new states accessible from the oxidized species along edge c and c'. This last stimulus is not directly reversible but a reduction can be used as a reset since pyrazine doesn't bind the neutral tweezers. In conclusion, the supramolecular concepts of mechanical motion and guest binging (molecular recognition) were combined in a molecular tweezers with the fascinating Ni-salen redox features to implement a reversible six-state system in which all states are stable and can be accessed and interconverted by the right combination of stimuli.

EXPERIMENTAL SECTION

EPR. EPR measurements were performed with a Bruker Elexsys spectrometer, at X-Band frequency, in the 4K to 300K temperature range. The magnetic field was modulated with a frequency of 100 kHz. $CHCl_3$ was dried over molecular sieves 4 Å, neutralized on Al_2O_3, and degased by argon bubbling. Distilled or spectrograde H_3CCN was used. Solutions of tweezers, metals, or ligands, were prepared in volumetric flasks, then degased by argon bubbling for 20 min. Solution additions were performed with Hamilton syringes. The X band perpendicular mode EPR measurements have been performed in Suprasil quartz tube (diameter 2 mm), on frozen and degased solutions (150 µL, 1.0 × 10^{-4} M).

Electrochemistry. Cyclic voltammetry (CV) and Differential pulse voltammetry (DPV) were performed on an Autolab potentiometer equipped with a differential electrometer amplifier PGSTAT100. Distilled or spectrograde H_3CCN were used, and CH_2Cl_2 was distilled over CaH_2. Solutions of metal salts

and ligands, were prepared in volumetric flasks. Solutions additions were performed with Hamilton syringes. Experiments were performed under Argon on 5 mL solutions of tweezers (2.0×10^{-4} M), with $TBAPF_6$ (0.1 M) as supporting electrolyte, in CH_2Cl_2. For closing solutions of metals were added (1.5 eq, 15 µL of 0.1 M solution in H_3CCN). For intercalation solution of pyrazine were added (1 eq ⇔10 µL, of 0.1 M solution in CH_2Cl_2). Electrolysis were performed on a Pt grid at room temperature under Argon. In a typical procedure: a solution of tweezers **1** (2.2 mg, 1.0×10^{-4} M) and $TBAPF_6$ (0.1 M) in CH_2Cl_2 (15 mL), was electrolyzed during 45 min with an applied potential of 1.2 V vs SCE. Spectroelectrochemistry was performed at room temperature using BASI spectroelectrochemical cell (1 mm path, WE: Pt grid, CE: Pt, Ref: Ag/AgCl) on Ar purged solutions.

General procedures. ^{1}H NMR and ^{13}C NMR spectra were recorded at 400 or 600 MHz on Bruker Avance III spectrometers. Reagent grade tetrahydrofuran was distilled from sodium and benzophenone. Tetrahydrofuran and triethylamine were degassed by three freeze-pump-thaw cycles before being used in the Sonogashira coupling reactions. All others chemicals were purchased from commercial suppliers and used without further purification. Flash column chromatography was performed using silica gel from Merck (40-63 µm) or GraceResolv High Resolution Flash Cartridges (particle size 40 µm). Thin layer chromatography was performed using aluminium plates pre-coated with silica gel 60 F254 0.20 mm layer thickness purchased from VWR. Absorption spectra were recorded on a JASCO V-670 spectrophotometer. Infrared spectra were recorded on a Brucker tensor 27 ATR spectrometer. Electrospray ionisation (ESI) mass spectrometry was performed on a Bruker microTOF spectrometer.

Complex 4. In a round bottom flask were introduced 4-bromo-1,2-diaminobenzene (400 mg, 2.14 mmol, 1 eq), 3,5-diterbutyl-2-hydroxybenzaldehyde **3** (1.05 g, 4.49 mmol, 2.1 eq), $Ni(OAc)_2$ (586 mg, 2.35 mmol, 1.1 eq), and absolute ethanol (20 mL). After heating the mixture at reflux during 15 h, a red precipitate was filtered, then dissolved in dichloromethane and passed through a plug of silica gel. The solvent was evaporated under reduced pressure yielding 81 % (1.17 g) of complex **4** as a red solid. ^{1}H NMR: (400 MHz, $CDCl_3$) δ 8.18 (s, 1H), 8.15 (s, 1H), 7.83 (d, J = 2.0 Hz, 1H), 7.58 (d, J = 8.8 Hz, 1H), 7.43 (d, J = 2.9 Hz, 1H), 7.42 (d, J = 2.9 Hz, 1H), 7.30 (dd, J = 8.8, 1.8 Hz, 1H), 7.10 (d, J = 2.6 Hz, 1H), 7.08 (d, J = 2.6 Hz, 1H), 1.46 (s, 18H), 1.31 (s, 9H), 1.30 (s, 9H); ^{13}C NMR (101 MHz, $CDCl_3$) δ 165.69, 165.31, 154.38, 154.14, 144.09, 142.18, 141.06, 140.98, 137.48, 137.36, 131.36, 131.14, 129.08, 126.78, 126.62, 119.73, 119.57, 119.55, 117.68, 115.34, 36.08, 34.14, 34.11, 31.31, 29.84; ESI-HRMS m/z (%): $[M+Na]^+$ calc ($C_{36}H_{45}BrN_2NiO_2Na$): 699.1889 (100), found: 699.1913 (100); Elemental analysis calc (%) for $C_{36}H_{45}BrN_2NiO_2$: C 63.93, H 6.71, N 4.14; found: C 63.80, H 6.79, N 4.16.

Complex 5. In a Schlenk tube under argon were introduced **4** (400 mg, 0.591 mmol, 1 eq), $PdCl_2(PPh_3)_2$ (62 mg, 0.089 mmol, 15 mol %), CuI (34 mg, 0.177 mmol, 30 mol %). A mixture of NEt_3 (6 mL) and THF (12 mL) previously distilled and degased was then added. The mixture was heated at 70°C, and TMSA (0.67 mL, 4.73 mmol, 8 eq) was added. The mixture was heated under argon at 70°C for 15 h. The solvent was evaporated under reduced pressure, and the crude product was purified by column chromatography (SiO_2: Cyclohexane / AcOEt (0-5 %)) yielding **5** as a red solid (308 mg, 75 %). ^{1}H NMR: (400 MHz, $CDCl_3$) δ 8.22 (s, 1H), 8.19 (s, 1H), 7.79 (d, J = 1.6 Hz, 1H), 7.64 (d, J = 8.7 Hz, 1H), 7.43 (d, J = 2.5 Hz, 1H), 7.41 (d, J = 2.5 Hz, 1H), 7.29 (dd, J = 8.6, 1.6 Hz, 1H), 7.11 (d, J = 2.6 Hz, 1H), 7.08 (d, J = 2.6 Hz, 1H), 1.46 (s, 9H), 1.45 (s, 9H), 1.31 (s, 9H), .30 (s, 9H), 0.28 (s, 9H); ^{13}C NMR (101 MHz, CDCl3) δ 165.49, 165.34, 154.45, 154.28, 143.12, 142.76, 141.04, 140.96, 137.33, 137.29, 131.14, 131.08, 130.09, 126.81, 126.59, 121.13, 119.65, 119.59, 117.85, 114.31, 104.14, 96.13, 36.07, 34.11, 31.34, 29.84, 0.10; ESI-HRMS m/z (%): $[M+Na]^+$ calc ($C_{41}H_{54}N_2NiO_2SiNa$): 715.3200 (100), found: 715.3225 (100).

Complex 6. In a round bottom flask, **5** (163 mg, 0.235 mmol, 1eq) was dissolved in a mixture of THF (10 mL) and MeOH (10 mL) and K_2CO_3 (65 mg, 0.47 mmol, 2eq) was added. The mixture was stirred at room temperature during 3 h. The solvent was evaporated under reduced pressure, and the red crude product was purified by plug filtration (SiO_2, CH_2Cl_2). After evaporated, **6** was obtained as a red solid (139 mg, 95 %). ^{1}H NMR: (400 MHz, $CDCl_3$) δ 8.21 (s, 1H), 8.20 (s, 1H), 7.83 (d, J = 1.5 Hz, 1H), 7.66 (d, J = 8.6 Hz, 1H), 7.43 – 7.42 (m, 2H), 7.31 (dd, J = 8.5, 1.5 Hz, 1H), 7.11 (d, J = 2.6 Hz, 1H), 7.08 (d, J = 2.5 Hz, 1H), 3.17 (s, 1H), 1.46 (s, 18H), 1.31 (s, 9H), 1.30 (s, 9H); ^{13}C NMR (101 MHz, CDCl3) δ 165.56, 165.42, 154.43, 154.40, 143.41, 142.81, 141.05, 140.98, 137.39, 137.34, 131.22, 131.15, 130.12, 126.79, 126.63, 120.05, 119.65, 119.58, 118.12, 114.41, 82.88, 78.68, 36.07, 34.11, 31.31, 29.84; ESI-HRMS m/z (%): $[M+Na]^+$ calc ($C_{38}H_{46}N_2NiO_2Na$): 643.2805 (100), found: 643.2784 (100); Elemental analysis calc (%) for $C_{38}H_{46}N_2NiO_2$: C 73.44, H 7.46, N 4.51; found: C 72.90, H 7.62, N 4.47.

Tweezers 1. In a Schlenk tube under argon were introduced 6,6″-Dibromo-2,2′:6′,2″-terpyridine **7** (24 mg, 0.060 mmol, 1eq), complex **6** (150 mg, 0.241 mmol, 4 eq), $PdCl_2(PPh_3)_2$ (8 mg, 0.012 mmol, 20 mol%), CuI (5 mg, 0.024 mmol, 40 mol%). A mixture of NEt_3 (4 mL) / THF (8 mL) previously distilled and degased was then added. The mixture was stirred at 70°C under argon during 24 h. After solvent evaporation the crude product was dissolved in CH_2Cl_2 and 4 drops of tris(2-aminoethyl)amine were added. The mixture was then washed by water (3 × 50 mL), dried over $MgSO_4$, filtrated, and evaporated. The red crude product was finally purified by column chromatography (SiO_2: CH_2Cl_2) yielding 65 % (58 mg) of tweezers **1** as a red solid. ^{1}H NMR: (400 MHz, $CDCl_3$) δ 8.61 (d, J = 6.3 Hz, 2H), 8.59 (d, J = 7.7 Hz, 2H), 8.28 (s, 2H), 8.24 (s, 2H), 8.09 – 7.98 (m, 3H), 7.90 (t, J = 7.8 Hz, 2H), 7.73 (d, J = 8.6 Hz, 2H), 7.61 (dd, J = 7.6, 1.1 Hz, 2H), 7.47 (d, J = 8.6 Hz, 2H), 7.44 (d, J = 2.4 Hz, 2H), 7.43 (d, J = 2.6 Hz, 2H), 7.14 (d, J = 2.4 Hz, 2H), 7.10 (d, J = 2.6 Hz, 2H), 1.48 (s, 18H), 1.47 (s, 18H), 1.33 (s, 18H), 1.32 (s, 18H). The material was not soluble enough for ^{13}C analysis. ESI-HRMS m/z (%): $[M+H]^+$ calc ($C_{91}H_{100}N_7Ni_2O_4$): 1472.6502 (100), found: 1472.6545 (100)

Half-tweezers 2. In a Schlenk tube under argon were introduced 6,6″-Dibromo-2,2′:6′,2″-terpyridine **7** (34 mg, 0.086 mmol, 1eq), complex **6** (134 mg, 0.216 mmol, 2.5 eq), $PdCl_2(PPh_3)_2$ (12 mg, 0.017 mmol, 20 mol%), CuI (7 mg, 0.035 mmol, 40 mol%). A mixture of NEt_3 (4 mL) / THF (8 mL) previously distilled and degased was then added. The mixture was stirred at 70°C under argon during 15 h. After solvent evaporation, the red crude products were separated by column chromatography (SiO_2: Cyclohexane / CH_2Cl_2 (0 – 100 %)) yielding 31 % (25 mg) of **2** as a red solid. ^{1}H NMR: (400 MHz, $CDCl_3$) δ 8.58 (dd, J = 7.7, 0.9 Hz, 1H), 8.57 (dd, J

= 7.9, 1.0 Hz, 2H), 8.48 (dd, J = 7.8, 1.1 Hz, 1H), 8.28 (s, 1H), 8,23 (s, 1H), 8.00 (d, J = 1.6 Hz, 1H), 7.98 (t, J = 7.8 Hz, 1H), 7.88 (t, J = 7.8 Hz, 1H), 7.73 (d, J = 8.7 Hz, 1H), 7.72 (t, J = 7.8 Hz, 1H), 7.60 (dd, J = 7.7, 1.1 Hz, 1H), 7.52 (dd, J = 7.9, 0.9 Hz, 1H), 7.47 (dd, J = 8.5, 1.5 Hz, 1H), 7.44 (d, J = 2.5 Hz, 1H), 7.43 (d, J = 2.5 Hz, 1H), 7.14 (d, J = 2.6 Hz, 1H), 7.10 (d, J = 2.6 Hz, 1H), 1.47 (s, 18H), 1.33 (s, 9H), 1.32 (s, 9H); ^{13}C NMR (101 MHz, $CDCl_3$) δ 165.68, 165.46, 157.47, 156.76, 154.91, 154.58, 154.40, 153.93, 143.58, 143.00, 142.67, 141.78, 141.10, 141.02, 139.29, 138.20, 137.48, 137.41, 137.22, 131.29, 131.20, 130.15, 130.04, 128.22, 127.50, 126.83, 126.67, 122.19, 121.93, 120.75, 120.29, 119.91, 119.73, 119.65, 118.19, 114.51, 90.42, 88.21, 36.08, 34.12, 31.30, 29.85; ESI-HRMS m/z (%): $[M+Na]^+$ calc ($C_{53}H_{54}BrN_5NiO_2Na$): 954.2687 (100), found: 954.2710 (100).

XRD crystal structures. CCDC 1537780 - 1537781, contain the supplementary crystallographic data for this paper. These data can be obtained free of charge from The Cambridge Crystallographic Data Centre via www.ccdc.cam.ac.uk/data_request/cif.

*Half-tweezers **2**.* Single crystals were grown by slow evaporation of $CHCl_3$ of **2**. Red plates-like crystals were obtained: $C_{54}H_{56}BrCl_2N_5NiO_2$, orthorhombic, Pca21, a = 41.7129(8), b = 7.09050(10), c = 17.3156(3) Å, α = β = γ = 90°, V = 5121.35(15) Å^3, Z = 4, T = 200(2) K. 6416 reflections measured, 6024 observed [$I \geq 2\sigma(I)$], 571 parameters, final R indices R_1 [$I \geq 2\sigma(I)$] = 0.0491 and wR_2 (all data)= 0.1373, GOF = 1.057.

*[Zn(**1**)]Cl_2.* Single crystals were grown by slow evaporation of chloroform/acetonitrile (8/2) of [Zn(**1**)]Cl_2. Brown plates-like crystals were obtained: $C_{95.25}H_{104.25}Cl_{8.75}N_8Ni_2O_4Zn$, monoclinic, I2/a, a = 35.3839(4), b = 11.1376(2), c = 51.7427(9) Å, α = γ = 90°, β = 95.8060(10)°, V = 20286.8(6) Å^3, Z = 8, T = 100(2) K. 28744 reflections measured, 19510 observed [$I \geq 2\sigma(I)$], 1189 parameters, final R indices R_1 [$I \geq 2\sigma(I)$] = 0.0863 and wR_2 (all data)= 0.2893, GOF = 1.044.

ASSOCIATED CONTENT

Supporting Information. NMR Spectra, DFT calculation, crystallographic data. This material is available free of charge via the Internet at http://pubs.acs.org.

AUTHOR INFORMATION

Corresponding Author

bernold.hasenknopf@upmc.fr; guillaume.vives@upmc.fr

Funding Sources

ANR JCJC SMARTEES (15-CE07-0006-01)
No competing financial interests have been declared.

ACKNOWLEDGMENT

BD thanks the Ecole Normale Supérieure de Cachan for a PhD Fellowship. Dr Sébastien Blanchard (UPMC) is warmly acknowledged for fruitful discussions. We are grateful to Dr P. Fertey (CRISTAL beamline team, synchrotron SOLEIL) and Dr S. Pillet (CRM2, Nancy) for their kind help in the collection of SC-XRD data. Financial support from the ANR SMARTEES (15-CE07-0006-01) is acknowledged. E.R. thanks the Spanish *Ministerio de Economía y Competitividad* for the grant CTQ2015-64579-C3-1-P and the Generalitat de Catalunya for an ICREA Academia grant. E.R. acknowledges BSC (Barcelona Supercomputer Center) for computational resources.

REFERENCES

1. (a) Kay, E. R.; Leigh, D. A.; Zerbetto, F., *Angew. Chem. Int. Ed.* **2007,** *46*, 72-191; (b) Balzani, V.; Venturi, M.; Credi, A., *Molecular Devices and Machines: Concepts and Perspectives for the Nanoworld*. Wiley-VCH: Weinheim: 2008; (c) Erbas-Cakmak, S.; Leigh, D. A.; McTernan, C. T.; Nussbaumer, A. L., *Chem. Rev.* **2015,** *115*, 10081-10206.

2. (a) Eelkema, R.; Pollard, M. M.; Vicario, J.; Katsonis, N.; Ramon, B. S.; Bastiaansen, C. W. M.; Broer, D. J.; Feringa, B. L., *Nature* **2006,** *440*, 163-163; (b) Vives, G.; Tour, J. M., *Acc. Chem. Res.* **2009,** *42*, 473-487; (c) Perera, U. G. E.; Ample, F.; Kersell, H.; Zhang, Y.; Vives, G.; Echeverria, J.; Grisolia, M.; Rapenne, G.; Joachim, C.; Hla, S. W., *Nature Nanotech.* **2013,** *8*, 46-51; (d) Kudernac, T.; Ruangsupapichat, N.; Parschau, M.; Macia, B.; Katsonis, N.; Harutyunyan, S. R.; Ernst, K. H.; Feringa, B. L., *Nature* **2011,** *479*, 208-211; (e) Lewandowski, B.; De Bo, G.; Ward, J. W.; Papmeyer, M.; Kuschel, S.; Aldegunde, M. J.; Gramlich, P. M. E.; Heckmann, D.; Goldup, S. M.; D'Souza, D. M.; Fernandes, A. E.; Leigh, D. A., *Science* **2013,** *339*, 189-193; (f) Zigon, N.; Guenet, A.; Graf, E.; Hosseini, M. W., *Chem. Commun.* **2013,** *49*, 3637-3639.

3. Browne, W. R.; Feringa, B. L., *Molecular Switches*. Wiley-VHC: Weinheim 2011; p XVII-XVIII.

4. Shankar, S.; Lahav, M.; van der Boom, M. E., *J. Am. Chem. Soc.* **2015,** *137*, 4050-4053.

5. (a) Green, K. A.; Cifuentes, M. P.; Corkery, T. C.; Samoc, M.; Humphrey, M. G., *Angew. Chem. Int. Ed.* **2009,** *48*, 7867-7870; (b) Akita, M., *Organometallics* **2011,** *30*, 43-51; (c) Vlasceanu, A.; Andersen, C. L.; Parker, C. R.; Hammerich, O.; Morsing, T. J.; Jevric, M.; Lindbæk Broman, S.; Kadziola, A.; Nielsen, M. B., *Chem. Eur. J.* **2016,** *22*, 7514-7523; (d) Liu, C.-G.; Su, Z.-M.; Guan, X.-H.; Muhammad, S., *J. Phys. Chem. C* **2011,** *115*, 23946-23954; (e) Szaloki, G.; Sevez, G.; Berthet, J.; Pozzo, J. L.; Delbaere, S., *J. Am. Chem. Soc.* **2014,** *136*, 13510-3; (f) Simao, C.; Mas-Torrent, M.; Casado-Montenegro, J.; Oton, F.; Veciana, J.; Rovira, C., *J. Am. Chem. Soc.* **2011,** *133*, 13256-9; (g) Basílio, N.; Cruz, L.; de Freitas, V.; Pina, F., *J. Phys. Chem. B* **2016,** *120*, 7053–7061; (h) Bakkar, A.; Cobo, S.; Lafolet, F.; Roldan, D.; Saint-Aman, E.; Royal, G., *J. Mater. Chem. C* **2016,** *4*, 1139-1143.

6. (a) Petitjean, A.; Kyritsakas, N.; Lehn, J. M., *Chem. Eur. J.* **2005,** *11*, 6818-28; (b) McConnell, A. J.; Wood, C. S.; Neelakandan, P. P.; Nitschke, J. R., *Chem. Rev.* **2015,** *115*, 7729-7793; (c) Machan, C. W.; Adelhardt, M.; Sarjeant, A. A.; Stern, C. L.; Sutter, J.; Meyer, K.; Mirkin, C. A., *J. Am. Chem. Soc.* **2012,** *134*, 16921-16924; (d) Lifschitz, A. M.; Young, R. M.; Mendez-Arroyo, J.; Stern, C. L.; McGuirk, C. M.; Wasielewski, M. R.; Mirkin, C. A., *Nat. Commun.* **2015,** *6*, 6541; (e) Lifschitz, A. M.; Rosen, M. S.; McGuirk, C. M.; Mirkin, C. A., *J. Am. Chem. Soc.* **2015,** *137*, 7252-7261; (f) Fermi, A.; Bergamini, G.; Roy, M.; Gingras, M.; Ceroni, P., *J. Am. Chem. Soc.* **2014,** *136*, 6395-6400; (g) Park, K. M.; Murray, J.; Kim, K., *Acc. Chem. Res.* **2017,** *50*, 644-646.

7. (a) Leblond, J.; Petitjean, A., *ChemPhysChem* **2011,** *12*, 1043-1051; (b) Hardouin-Lerouge, M.; Hudhomme, P.; Salle, M., *Chem. Soc. Rev.* **2011,** *40*, 30-43; (c) Klärner, F.-G.; Kahlert, B., *Acc. Chem. Res.* **2003,** *36*, 919-932; (d) Zimmerman, S., *Top. Curr. Chem.* **1993,** *165*, 71-102.

8. (a) Doistau, B.; Tron, A.; Denisov, S. A.; Jonusauskas, G.; McClenaghan, N. D.; Gontard, G.; Marvaud, V.; Hasenknopf, B.; Vives, G., *Chem. Eur. J.* **2014,** *20*, 15799-15807; (b) Doistau, B.; Rossi-Gendron, C.; Tron, A.; McClenaghan, N. D.; Chamoreau, L.-M.; Hasenknopf, B.; Vives, G., *Dalton Trans.* **2015,** *44*, 8543-8551.

9. (a) Kurahashi, T.; Fujii, H., *J. Am. Chem. Soc.* **2011,** *133*, 8307-8316; (b) Rotthaus, O.; Jarjayes, O.; Thomas, F.; Philouze, C.; Perez Del Valle, C.; Saint-Aman, E.; Pierre, J.-L., *Chem. Eur. J.* **2006,** *12*, 2293-2302; (c) Benisvy, L.; Kannappan, R.; Song, Y.-F.; Milikisyants, S.; Huber, M.; Mutikainen, I.; Turpeinen, U.; Gamez, P.; Bernasconi, L.; Baerends, E. J.; Hartl, F.; Reedijk, J., *Eur. J. Inorg. Chem.* **2007,** *2007*, 637-642.

10. Rotthaus, O.; Thomas, F.; Jarjayes, O.; Philouze, C.; Saint-Aman, E.; Pierre, J.-L., *Chem. Eur. J.* **2006,** *12*, 6953-6962.

11. Neufeld, R.; Stalke, D., *Chem. Sci.* **2015,** *6*, 3354-3364.

12. Shimazaki, Y.; Tani, F.; Fukui, K.; Naruta, Y.; Yamauchi, O., *J. Am. Chem. Soc.* **2003,** *125*, 10512-10513.

13. Shih, H.-W.; Dong, T.-Y., *Inorg. Chem. Commun.* **2004,** *7*, 646-649.

14. (a) Kochem, A.; Gellon, G.; Leconte, N.; Baptiste, B.; Philouze, C.; Jarjayes, O.; Orio, M.; Thomas, F., *Chem. Eur. J.* **2013,** *19*, 16707-16721; (b) Storr, T.; Verma, P.; Shimazaki, Y.; Wasinger, E. C.; Stack, T. D. P., *Chem. Eur. J.* **2010,** *16*, 8980-8983; (c) Lecarme, L.; Chiang, L.; Philouze,

C.; Jarjayes, O.; Storr, T.; Thomas, F., *Eur. J. Inorg. Chem.* **2014,** *2014*, 3479-3487.

15. Diallo, A. K.; Absalon, C.; Ruiz, J.; Astruc, D., *J. Am. Chem. Soc.* **2011,** *133*, 629-641.

16. (a) Glaser, T.; Heidemeier, M.; Fröhlich, R.; Hildebrandt, P.; Bothe, E.; Bill, E., *Inorg. Chem.* **2005,** *44*, 5467-5482; (b) Storr, T.; Wasinger, E. C.; Pratt, R. C.; Stack, T. D. P., *Angew. Chem. Int. Ed.* **2007,** *46*, 5198-5201.

17. Blum, V.; Gehrke, R.; Hanke, F.; Havu, P.; Havu, V.; Ren, X.; Reuter, K.; Scheffler, M., *Comput. Phys. Commun.* **2009,** *180*, 2175-2196.

18. Perdew, J. P.; Burke, K.; Ernzerhof, M., *Phys. Rev. Lett.* **1996,** *77*, 3865-3868.

19. Becke, A. D., *J. Chem. Phys.* **1993,** *98*, 5648-5652.

20. (a) Ruiz, E.; Cano, J.; Alvarez, S.; Alemany, P., *J. Comput. Chem.* **1999,** *20*, 1391-1400; (b) Adamo, C.; Barone, V.; Bencini, A.; Broer, R.; Filatov, M.; Harrison, N. M.; Illas, F.; Malrieu, J. P.; Moreira, I. d. P. R., *J. Chem. Phys.* **2006,** *124*, 107101.

Table of Contents